

DPPH Free Radical Scavenging Activity, and their Synthetic, Structural, Electronic and Magnetic Studies of Two [Cu^{II}₂(thb)] Compounds, (thb = *N,N,N',N'*-tetrakis-{3-[(2-hydroxybenzylidene)-amine]propyl}-1,4-butanodiamine)}

Elizabeth Baca-Solis¹, Marcos Flores-Alamo², Daniel Ramírez-Rosales³, Rafael Zamorano-Ulloa³, Samuel Hernández-Anzaldo¹ and Yasmi Reyes-Ortega^{1*}

¹Instituto de Ciencias, Centro de Química, BUAP, Edif. 103H, Complejo de Ciencias, CU, Col. San Manuel, Puebla, C.P. 72570, México

²Facultad de Química, Universidad Nacional Autónoma de México, Ciudad Universitaria, México D. F. 04510, México

³Escuela Superior de Física y Matemáticas-IPN Av. Instituto Politécnico Nacional, Edif. 9 Unidad Profesional Adolfo López Mateos, Zacatenco, Delegación Gustavo A. Madero, México

Abstract

Synthesis, structural, electronic, and magnetic characterization of two [Cu^{II}₂(thb)] (thb = *N,N,N',N'*-tetrakis-{3-[(2-hydroxybenzylidene)-amine]propyl}-1,4-butanodiamine)}) crystalline phases (**1a** and **1b**) are reported. Both, **1a** and **1b**, showed free radical scavenging activity, which was quantified by the DPPH free radical scavenging activity assay. **1b** crystallized in a P2₁/c space group. In **1b** each molecule contains two Cu^{II}-(hidroxibenzylidene) groups bonded in the extremes of the organic DAB-Am nucleus. The Cu^{II}-(hidroxibenzylidene) groups of each extreme, form 1D chains along of the *b*-axis. IR and UV-Vis spectra showed *d-d* transitions and $\nu_{\text{Cu-O}}$, $\nu_{\text{Cu-N}}$ vibrations respectively, confirming the formation of the compound. ¹H-NMR spectra of **1a** and **1b** showed similar spectra, being characteristics of paramagnetic compounds. Bulk magnetization of **1a** and **1b** from 2 K to 300 K showed paramagnetic behaviour. The best fit for the susceptibility data was obtained using Curie-Weiss and modified Curie-Weiss equations with θ and C values of $\theta_{1a/1b \text{ C-W}} = 0 \pm 1 \text{ K}$, $C_{1a/1b \text{ C-W}} = 0.82/0.66 \text{ cm}^3 \text{ K mol}^{-1}$, and $\theta_{1a/1b \text{ modified C-W}} = 0.6 \pm 1 \text{ K}$ and $C_{1a/1b \text{ modified C-W}} = 0.80/0.70 \text{ cm}^3 \text{ K mol}^{-1}$. The X-band ESR spectra of **1a** and **1b** in solid samples showed a single and a rhombic signals, respectively, with *g* values around 2.1 at 77 K and 300 K, however, in CH₂Cl₂ solutions at 77 K the spectra were similar. The spectroscopic and magnetic results allowed us to conclude that **1a** and **1b** are two different crystalline phases which were proven to act as effective antioxidants showing both an IC₅₀ = 16.5 μM, in contrast with Trolox, IC₅₀ = 39.3 μM, normally used as a vitamine E analog and a strong antioxidant. Additionally the DPPH free radical is scavenged by reduction mechanism of Cu^{II} to Cu^I. The overall electronic, magnetic and structural information about **1a** and **1b** provide us some characteristics of this kind of transitional metal ionic coordination compounds.

Keywords: Antioxidant activity; Branched Cu^{II}-polymer complexes; Structural, electronic and magnetic studies

Introduction

Branched polymers are three-dimensional molecular structures, which have transformed the classic polymer concept, leading to develop a new field in chemistry [1-18]. In the biological world, dendritic molecules are present at different length scales, while in synthetic chemistry, there are many possibilities to synthesize branched macromolecules by changing the terminal groups of the different cores obtained. This strategy has allowed the modification of some physical and chemical properties and it has been applied to obtain a large number of new families of polymers with diverse applications [3-18]. Particularly, the poly(propyleneimine) (PPI) is one of the first families of commercially available synthetic dendrimers with a well-defined structure that can be functionalized up to the 64th generation. The PPI core is 1,4-diaminobutane (DAB) which has been transformed to 4, 8, 16, 32 and 64 generations, containing the same number of terminal amine (Am) groups [1,2]. So far, the spatial treats of these highly mobile molecules have been inferred; however, the spatial structures are still unknown. Importantly the covalent dendrimers structures have shown interesting applications, such as, antibacterial [6], nanoparticles containing metals [7-14], catalysts for different reactions [13,14], metal-encapsulators [14-18], nanoparticles templates for growing carbon nanotubes [18], among others. Hence our interest in this molecular polymer. We previously report the preparation and characterization of the branched ligand *N,N,N',N'*-tetrakis-{3-[(2-hydroxybenzylidene)-amine]propyl}-1,4-butanodiamine) thb [19], used here to obtain a Cu^{II}

complex in two different crystalline phases, [Cu^{II}₂(thb)] **1a** and **1b**, both characterized electronic and magnetically, with considerably good antioxidant activity as shown below resolving, the **1b** spatial structure. Herein, the scavenging activity of [Cu^{II}₂(thb)] is studied, using the known free scavenging assay with the stable radical DPPH by UV-Vis [20]. The antioxidant activity relationship of coordination compounds containing transitional metals ions, like Copper and Chromium, has been proven in both, *in vitro* and *in vivo* models, for example, 1,1-diphenyl-2-picrylhydrazyl (DPPH) kinetic analysis, γ -radiolysis of rat liver microsomes, 2,2-azobis(2-amidinopropane)dihydrochloride (AAPH)-induced low density lipoprotein (LDL) oxidation, as well, AAPH-induced linoleic oxidation. Free radicals are, in most cases, produced physiologically by the cells. One example is the formation

*Corresponding author: Yasmi Reyes Ortega, Centro de Química del Instituto de Ciencias, Benemérita Universidad Autónoma de Puebla, Edif. F103 Complejo de Ciencias, Ciudad Universitaria, Col. San Manuel, Puebla, Pue. 72570, México, Tel: (222)2295500 extn. 7292; E-mail: yasmi.reyes@correo.buap.mx

Received March 26, 2016; Accepted April 14, 2016; Published April 21, 2016

Citation: Baca-Solis E, Flores-Alamo M, Ramírez-Rosales D, Zamorano-Ulloa R, Hernández-Anzaldo S, et al. (2016) DPPH Free Radical Scavenging Activity, and their Synthetic, Structural, Electronic and Magnetic Studies of Two [Cu^{II}₂(thb)] Compounds, (thb = *N,N,N',N'*-tetrakis-{3-[(2-hydroxybenzylidene)-amine]propyl}-1,4-butanodiamine)}. J Anal Bioanal Tech 7: 315. doi:10.4172/2155-9872.1000315

Copyright: © 2016 Baca-Solis E, et al. This is an open-access article distributed under the terms of the Creative Commons Attribution License, which permits unrestricted use, distribution, and reproduction in any medium, provided the original author and source are credited.

of the superoxide anion radical ($O_2^{\cdot-}$) which is formed during the mitochondrial respiratory chain reaction and the nitric oxide radical (NO) is made by the activation of nitric oxide synthase [21]. In some cases, the overproduction of radicals, as well as the formation of toxic radicals causes damage of biological molecules, resulting in many disease conditions. Oxidative stress is generated by the increase of free radical production and it has been linked to inflammatory processes. Hence, coordination compounds with radical scavenging activity are used to inhibit the free radical activity then to prevent several diseases [22].

Experimental Section

Materials and methods

1a, 1b solutions were prepared by dissolving crystalline samples. Electronic spectra were measured with a Shimadzu UV-3100S spectrophotometer at 298 K ($\lambda=200-1200$ nm) in CH_2Cl_2 solution and CH_3OH solutions for **1a, 1b**, at ca. $10^{-5}M$. A Nicolet Magna-IR 750 spectrophotometer ($\bar{\nu}=400-4000$ cm^{-1}) was employed to monitor the infrared spectra using KBr pellets. 1H - and ^{13}C -NMR spectra of **1** and only 1H -NMR of **1a, 1b** were recorded on a JEOL Eclipse-400 at rt using $CDCl_3$ solutions and TMS as reference. 1H -NMR study of **1a, 1b**, was carried out in a range from 100 to -100 ppm with acquisition time of 1 sec and 22000 repetitions. ESR spectra at X-band frequencies (9 GHz) for **1a, 1b** were obtained with a JEOL JES-RES 3X spectrometer, at different temperatures from 300 K to 77 K, on polycrystalline powder samples and using 2,2-diphenyl-1-picrylhydrazyl (DPPH) as primary standard. ESR spectra at 77 K of **1a, 1b** in CH_2Cl_2 solution using different concentrations (10^{-3} to $10^{-4}M$) were recorded with 2 min scan time, 1×0.1 mT modulation, 0.03 ms time constant, 1 mW power, 2.5×100 mT fieldwidth, 5×10 gain for **1a**; with 2 min scan time, 1×0.1 mT modulation, 0.03 ms time constant, 1 mW power, 1.5×100 mT fieldwidth, 4×10 gain for **1b**. X-band power variation experiment at 77 K for **1b** powder sample was carried out from 0.01 to 160 mW. Measurements were performed in a magnetic field of 1 kOe, in the range 2-300 K, using a gelatine capsule and a Quantum Design Magnetometer. Calculated Pascal constants for **1a, 1b** were about 264×10^{-6} emu.

General procedure for synthesis of compounds 1a, 1b

Synthesis of **1a, 1b** was carried out using the direct synthesis method [23,24]. A stoichiometric ratio of 2:1, Cu^0 0.6022 mmol:1 0.3011 mmol, respectively, and dimethylsulfoxide (2 ml) were placed in a flask. The reaction mixture is kept under stirring at rt for five days, and then filtered to give a green powder, which is dissolved in methanol. Green crystals are formed in the solution. The crystals of **1b** were separated manually. The yield for **1a** chloroform crystals is lower (yield: 30%) than that for **1b** methanol crystals (yield: 60%) and the latter are suitable for X-ray crystallography.

1a: mp 165°C; Found: C, 61.49; H, 6.07; N, 9.74. Calc. for $Cu_2C_{44}H_{52}N_6O_4$: C 61.8; H 6.08; N 9.82; UV-Vis $\lambda_{max}(CHCl_3)/nm$ ($\epsilon/M^{-1}cm^{-1}$), 224 (30848.33), 241 (28545.11), 262.61 (9989.74), 277.31 (11015.94), 290.23 (6220.03), 365 (6345.69), 447.57 (18.33), 648.31 (112.57), 811.39 (486.92), 959.02 (348.18); IR (KBr) $\bar{\nu}_{max}/cm^{-1}$, 447.4 and 426.2 (Cu-N), 470.5 (Cu-O), 1633.4 (C=N), 1600.7 (C=C); 1H -NMR $\delta(CDCl_3; (CH_3)_4Si)$: 89.09, 76.02, 54.74, 21.28, 8.89, 3.49, 2.62, 1.55, -25.96, -49.90, -54.74, -77.24, -86.75; ESR (powdered sample) at 300 K/77 K: 2.117/2.118; $\chi_M T$ at 182 K: 0.7181 $emu mol^{-1} K$ (spin only 0.3760 $emu mol^{-1} K$).

1b: mp 215°C; Found: C, 61.48; H, 6.05; N, 9.63. Calc. for $Cu_2C_{44}H_{52}N_6O_4$: C 61.8; H 6.08; N 9.82; UV-Vis $\lambda_{max}(CHCl_3)/nm$

($\epsilon/M^{-1}cm^{-1}$), 224 (31372.4), 239 (26073.85), 255.17 (11371.97), 276.52 (10722.74), 297.47 (5110.05), 364.72 (5487.02), 446.79 (20.94), 642.57 (194.71), 808.55 (277.49), 938.28 (193.72); IR (KBr) $\bar{\nu}_{max}/cm^{-1}$, 455.1 y 420.4 (Cu-N); 472.5 (Cu-O); 1635.4 (C=N); 1598.7 (C=C); 1H -NMR $\delta(CDCl_3; (CH_3)_4Si)$: 89.09, 76.02, 54.74, 21.28, 8.89, 3.49, 2.62, 1.55, -25.96, -49.90, -54.74, -77.24, -86.75; ESR (powdered sample) at 300 K/77 K: $g_1(300/77) = 2.190/2.192$, $g_2(300/77) = 2.101/2.103$, $g_3(300/77) = 2.053/2.052$; $\chi_M T$ at 200 K: 0.4630 $emu mol^{-1} K$ (spin only 0.3760 $emu mol^{-1} K$).

X-ray diffraction data of 1b

A green needle crystal mounted on glass fibre was studied with an Oxford Diffraction Gemini "A" diffractometer with a CCD area detector ($\lambda_{MoK\alpha} = 0.71073$ Å, monochromator: graphite) source equipped with a sealed tube X-ray source at 130 K. Unit cell constants were determined with a set of 15/3 narrow frame/runs (1° in) scans. A data sets consisted of 337 frames of intensity data collected with a frame width of 1° in , a counting time of 100 s/frame, and a crystal-to-detector distance of 55.00 mm. The double pass method of scanning used to exclude any noise. The collected frames integrated by using an orientation matrix determined from the narrow frame scans.

CrysAlisPro and CrysAlis RED software packages were used for data collection and data integration [25]. Analysis of the integrated data did not reveal any decay. Final cell parameters were determined by a global refinement of 6928 reflections ($\theta < 26^\circ$). Collected data were corrected for absorption effects by using analytical numeric absorption correction with a multifaceted crystal model based on expressions upon the Laue symmetry using equivalent reflections [26]. Structure solution and refinement were carried out with the programs: SHELXS97, SHELXL97 [27], and the software used to prepare material for publication was WinGX [28,29].

Full-matrix least-squares refinement was carried out by minimizing $(F_o^2 - F_c^2)^2$. All non-hydrogen atoms were refined anisotropically. The H atom (H-O) of the hydroxo group was located in a difference map and refined isotropically with $U_{iso}(H) = 1.5 U_{eq}$ for (O). H atoms attached to C atoms were placed in geometrically idealized positions and refined as riding on their parent atoms, with C-H = 0.95–0.99 Å and $U_{iso}(H) = 1.2U_{eq}(C)$, or $1.5 U_{eq}(C)$ for aromatic, methylene and methyl groups. Crystal data and experimental details of the structure determination listed in Table S3.

DPPH radical scavenging assay

The hydrogen donating or radical scavenging ability of $Cu^{II}_2(thb)$ was evaluated using a stable radical, 1,1-diphenyl-2-picryl hydrazyl (DPPH, Sigma, St. Louis, MO, USA). The reaction mixture was composed of 1.5 mL of 0.2 and 0.3 mM DPPH solution and 20 μL of the test compound in a total volume of 3 mL of methanolic solution. Stock solutions of $Cu^{II}_2(thb)$ were prepared in 100% methanol and the final concentrations ranged from 5–100 μM . This assay was performed in triplicate in the two different phases of the $Cu^{II}_2(thb)$ compound named 1a/1b and the free radical (thb) at 0.2 mM. The reaction mixtures were incubated at room temperature for 15 minutes then the solutions were measured by a Shimadzu UV-3100S spectrophotometer UV-Vis ($\lambda = 200-1100$ nm).

Results and Discussion

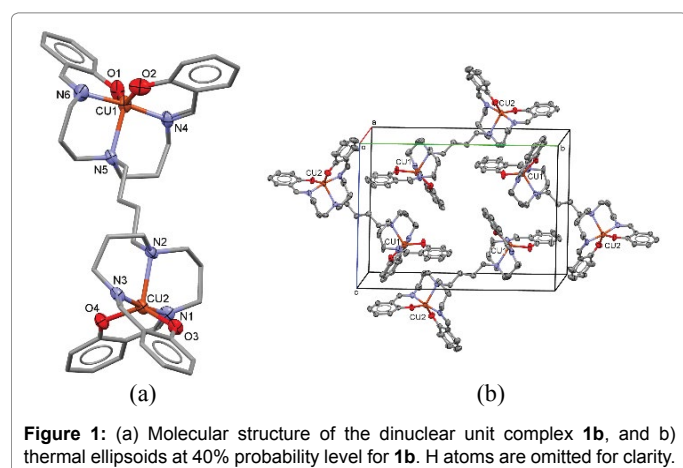
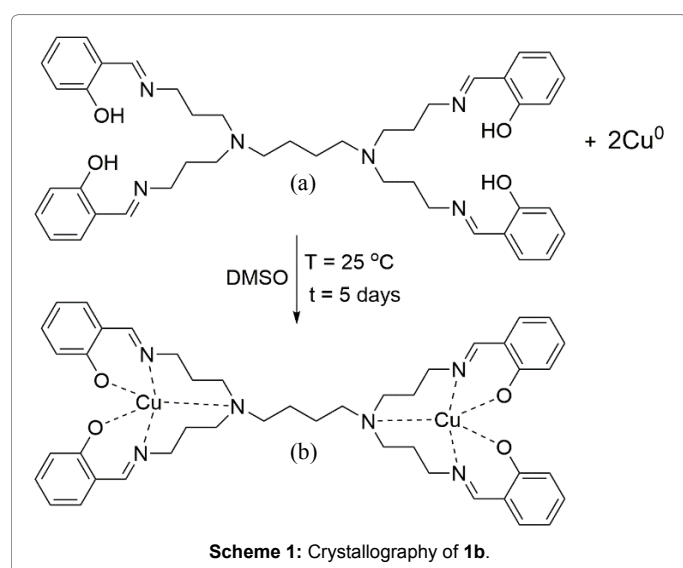
Synthesis of [Cu^{II}(thb)] 1a, 1b

The organic ligand *N,N,N',N'*-tetrakis-[(2-hydroxybenzyliden)-amine]propyl]-1,4-butanodiamine (thb) was synthesized as previously

reported [19]. **1a** and **1b** were obtained by direct synthesis method [18,23,24]. The absence of residual salts favours the formation of pure compounds, separated as solid samples from the reaction medium [24,30,31]. In the present work, this methodology has been essential in order to obtain two polymorphs of the complex [Cu₂^{II}(thb)], **1a** and **1b** (Scheme 1), one of which, **1b**, was obtained as a single crystal. The **1a** molecular structure must be the same as **1b** because in solution both gave the same spectroscopic response and the same antioxidant activity, but in solid state, the spectroscopic results are different, so we conclude that **1a** and **1b** contain the same molecules with different network arrangement.

Crystallography of **1b**

The asymmetric unit consists of two Cu^{II}-(hydroxybenzylidene) molecules of the **1b** compound. Four methanol crystallization solvent molecules stabilize to four dinuclear Cu^{II} complexes in the monoclinic crystal system with P2₁/c space group. The **1b** compound has two main coordination sites; each site contains two salen groups and a tertiary amine group, acting as a five-dentate ligand around the Cu^{II} ions, (Figure 1). The dinuclear unit geometry around each Cu^{II} ion can be described as an intermediary between a square-pyramidal (*sp*) and a trigonal bipyramidal (*tbp*) geometry, consistently with the geometric τ parameters of 0.58 found for Cu1 and of 0.63 for Cu2 [32,33]. Axially,



Cu1 is coordinated to N4 and N6, while Cu2 is coordinated to N1 and N3 of the imine groups. The equatorial plane around the Cu^{II} ions is formed by N5, O1 and O2 for Cu1, and by N2, O3 and O4 for Cu2. The longest bond distances are 2.345 (3) and 2.337 (3) Å for Cu-N5 and Cu2-N2 respectively.

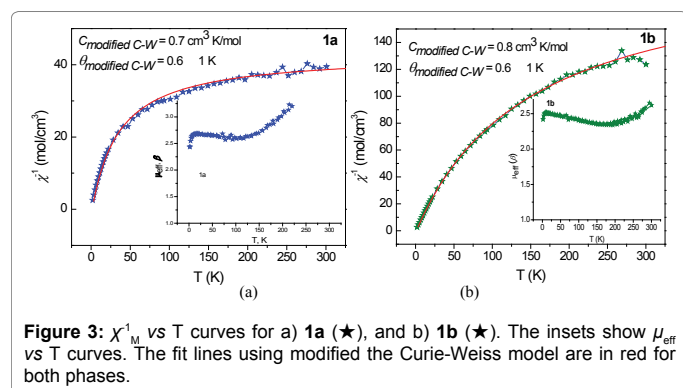
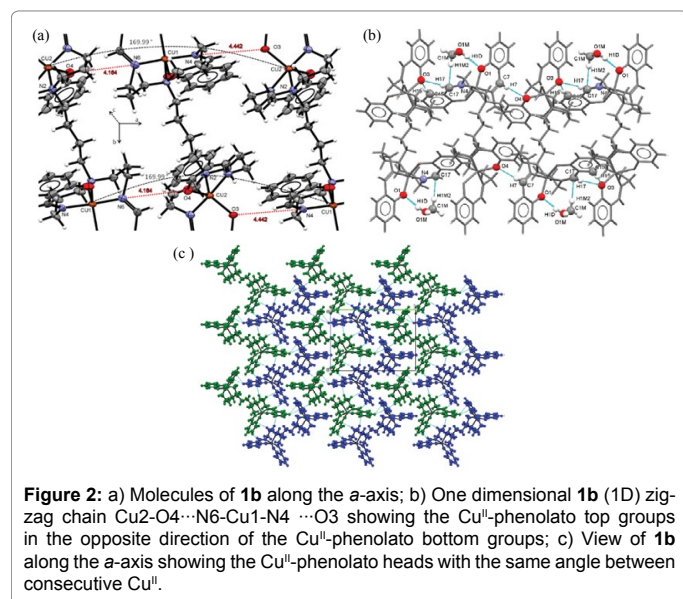
Intermolecular interactions of type O-H...H are observed on crystalline structure of **1b** which stabilize the network crystalline (Figure 2a): *i*) interactions between the hydrogen (H1D) atom of methanol solvent and the oxygen atom (O1) of thb, H1D...O1 (2.812(5) Å); *ii*) interactions between the thb hydrogen (H7) atom and the oxygen (O4) atom of a nearby thb molecule, H7...O4 (3.481(6) Å); *iii*) interactions between the thb hydrogen (H15) atom and the oxygen (O3) atom of a nearby thb molecule, H15...O3 (2.675(3) Å); *iv*) interactions between the thb hydrogen (H17) atom and the oxygen (O3) atom of a nearby thb molecule, H17...O3 (3.585(6) Å). All the interactions construct an infinite layer along the *a-b* plane, forming a three-dimensional supramolecular arrangement, (Figure 2c). The crystalline structure of **1b** consists of molecules parallel to the *b*-axis, which are stacked along the *a*-axis (Figure 2b-c).

Thb phenolato top heads form zig-zag chains due to the Cu2-O4...N6-Cu1 inter-dinuclear interactions [O4...N6 distance: 4.164(9) Å; N4...O3 distance: 4.442(4) Å], meanwhile the phenolato at the bottom heads of each Cu^{II}-thb molecule form zig-zag chains due to the Cu1-N6...O4-Cu2 inter-dinuclear interactions [O4...N6 distance: 4.164(9) Å; O3...N4 distance: 4.442(4) Å] (Figure 2c). Finally, the Cu-Cu intramolecular distance was 10.1391(9) Å maintaining the Cu ions isolated from each other [33,34].

UV-Vis and IR spectroscopy

The UV-Vis spectra of **1a** and **1b** (Supplementary information in Figure S1a, b), in CH₃OH solutions are very similar. The hydroxyl of the phenolate groups are deprotonated by coordination with the copper ion, therefore, they have two electron lone pairs, which showed one electronic transition in the UV-Vis spectra. On the other hand, the N lone electron pair is used to form the coordination bond with the copper ion. The other transitions are assigned to two metal-ligand charge transfer transitions and one ligand-metal charge transfer transition (Supplementary Information in Table S2). Supplementary Information inset in Figure S1 showed the $d_{xz}, d_{yz} \rightarrow d_z^2, d_{x^2-y^2} \rightarrow d_z^2$ and $d_{xy} \rightarrow d_z^2$ transitions for **1a** at 811 nm with shoulders at 648 nm and 959 nm, and for **1b** (inset in Figure 3a) at 808 nm, 642 nm and 938 nm. These transitions are characteristic of five-coordinated Cu^{II} compounds with distorted geometries [34-36]. The *d-d* transitions for **1a** and **1b** spectra helped to build an OM diagram, which is shown in Figure 3b. The oscillator strength, *f*, values for the *d-d* transitions were calculated and their energy values are among those found for *d-d* forbidden transitions and the reported values for energies corresponding to pure *sp* and pure *tbp* geometries [35,36]. The reported values for **1a** and **1b** showed in Supplementary information in Table S2 were very close. When **1a**, **1b** in methanol solutions were treated with NaBH₄ to Cu^I, the color of both solutions changed from green to brown, suggesting the formation of Cu^I-clusters. For these solutions the *d-d* and CT transitions in the UV-Vis spectra disappeared, and an exponential curve emerged, where the Mie Plasmon peak at 590 nm was not observed. Similar spectra were obtained for compounds with particle size < 5 nm and non-isolated Cu^I atoms; therefore, the molecule size of **1a** and **1b** were < 5 nm (Supplementary Information, in Figure S2) [7,10].

IR spectra of **1a** and **1b** are characteristic of metal transition compounds showing characteristic peaks of the thb, which shifted due



to the presence of Cu^{II} ions. The strong electronegative of Cu^{II} removes not only the electron density of the atoms in the first coordination sphere but also from neighbouring atoms through an inductive effect (Supplementary Information, in Figure S3a and b) [33,37]. Both spectra did not show the $\nu_{\text{O-H}}$ vibration peak indicating that the coordination of the phenol oxygen atoms to Cu^{II} as phenolato groups. This feature was in agreement with the **1a**, **1b** UV-Vis spectra, which did not show the two $n(\text{N}) \rightarrow \pi^*$ (imino-phenolato) transition bands, observed in the thb UV-Vis spectrum, and only one band corresponding to the $n(\text{O}) \rightarrow \pi^*$ (imino-phenolato) transition observed in the thb ligand UV-Vis spectrum [19].

¹H-NMR of **1a**, **1b**

Previously, our group reported ¹H-NMR studies of paramagnetic compounds with and without aromatic protons, which are very similar to the ¹H-NMR spectra of **1a**, **1b** [36-38]. Supplementary Information in Figure S4 showed the ¹H-NMR spectra with three important regions, showing different relaxation times. Two paramagnetic zones at downfield (100 to 10 ppm zone I) and one at upfield (-90 to -1 ppm, zone II), where the broad bands are contained; meanwhile the diamagnetic zone (0 to 10 ppm, zone III) contains narrower lines. In diamagnetic zone III, the signals correspond to the aromatic protons, which are outside of a sphere with radius >5 Å from the metal ions, while the broader lines in zones I, II in ¹H-NMR correspond to all protons within a sphere with average radius <5 Å from the metal ions. ¹H-NMR spectra

of **1a**, **1b** were characteristics of paramagnetic complexes, with broad lines due the dipolar relaxation and the hyperfine protons coupling, which were sufficiently close to the metal and/or for which electron spin nuclear spin relaxation times are shorter than 5 ns [39-44].

Magnetic measurements

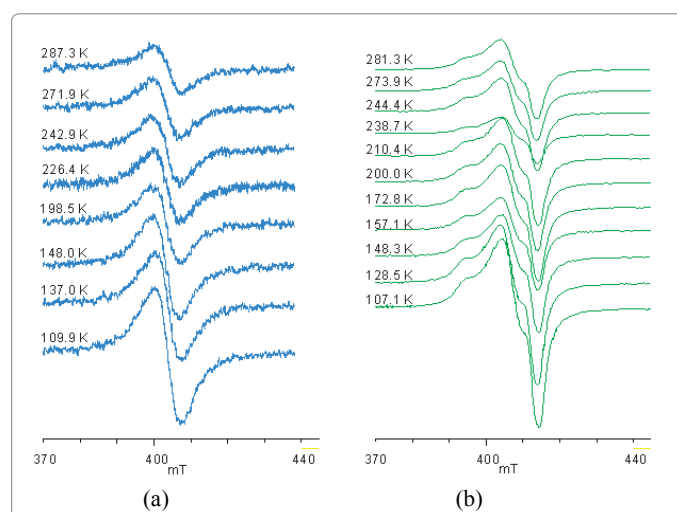
χ_M^1 vs *T* bulk measurements from 2 to 300 K are presented in Figure 3a, b. The linear behaviour of χ_M^1 vs *T*, in a temperature range of 2 to 83 K for **1a** and 2 K to 133 K for **1b**, shows that both phases are paramagnetic. Insets in Figure 3a, b, show the μ_{eff} vs *T* plots, indicating that the μ_{eff} values are temperature-independent between 13 K to 133 K for **1a** and between 11 K to 206 K for **1b**.

In order to have better insight of the magnetic behaviour of both compounds, different models for fitting the susceptibility were used, including the Ising [45], Bonner-Fisher [46], Myers [47] and Bleany-Bowers models [48]. A good fitting ($r^2 = 0.999$ for both compounds) was obtained using the Curie-Weiss model (C-W) [49], with constant values of $C_{1a/1b \text{ C-W}} = 0.82/0.66 \text{ cm}^3 \text{ K mol}^{-1}$ and Curie-Weiss temperature values of $\theta_{1a/1b \text{ C-W}} = 0 \pm 1 \text{ K}$, (Support Information, in Figure S5 a and b, red solid lines). However, the best fitting ($r^2 > 0.999$) for both compounds was obtained with a modified Curie-Weiss model (modified C-W) (eq 1) [50] (Figure 4a, b red solid lines), with Curie constant values of $C_{1a/1b \text{ modified C-W}} = 0.80/0.70 \text{ cm}^3 \text{ K mol}^{-1}$ and modified Curie-Weiss temperature values of $\theta_{1a/1b \text{ modified C-W}} = 0.6 \pm 1 \text{ K}$.

$$\chi_{\text{modified C-W}}(T) = \chi_{\text{modified C-W}} + \alpha T + \frac{C_{\text{modified C-W}}}{[T\{\theta_{\text{modified C-W}}|T\}^2 - (\theta_{\text{modified C-W}}|T)^3]} - \theta_{\text{modified C-W}} \quad (1)$$

where $\theta_{\text{modified C-W}}$ is a correction to the Curie-Weiss temperature, *T* is the temperature, αT is a phenomenological susceptibility and along with $\chi_{\text{modified C-W}}$ give the total Pascal constants. It is clear that the modified Curie-Weiss model fitted better, however, both models are adequate.

Regarding **1b**, the Cu^{II} ions in the dinuclear molecules were well separated as it was shown in the crystallographic section, therefore, the molecules can be considered as monomers as they are. The same conclusion can be applied for **1a**. The diamagnetic hydrocarbonated bridge supports the isolated ions, avoiding the intramolecular and intermolecular magnetic interactions, which is consistent with the magnetic studies.



ESR measurements

X-band ESR spectra for **1a**, **1b** in powder samples, were recorded at 77 K and 300 K (Supplementary information, in Figure S6). For any paramagnet the Zeeman interaction is expressed via the *g*-tensor which has three mutually orthogonal main values of *g*. The deviation of the *g*-values from free electron value ($g_e = 2.0023$) carries information about the orbital angular momentum of the electron and information about the electronic structure [50]. At 77 K/300 K **1a** ESR spectra (Figure S6a) showed a broad singlet with *g* value of $g^{77}/g^{300} = 2.118/2.117$. ESR of **1b** in power samples at 77 K/300 K (Supplementary information, in Figure S6b) showed a rhombic spectra with *g* values of $g_1^{77}/g_1^{300} = 2.192/2.190$, $g_2^{77}/g_2^{300} = 2.103/2.101$ and $g_3^{77}/g_3^{300} = 2.052/2.053$. All spectra did not show any additional resonances at zero field or at any other field. Neither hyperfine nor superhyperfine interactions were observed [49]. The obtained *g*-values of **1a**, **1b** are in agreement with those reported for Cu^{II}-dendrimers complexes [51-55]. In order to corroborate the rhombic spectrum for **1b**, we carried out power variation experiments in which all the spectra features increased at the same rate as the microwave power. These results clearly indicate the presence of only one Cu^{II} specie. (Supplementary Information, in Figure S7). The ESR spectra differences indicate that structurally there is a higher asymmetry for **1b** in the solid state. However, both spectra showed no well-define signals produced by magnetic interactions or by short relaxation times present in the samples [54,56,57]. It should be noted that *g* values for **1a**, **1b** did not change when the temperature was decreased to 77 K, this happens because the magnetic structure of the Cu^{II}-thb complex remains unchanged.

Furthermore, the sequences of powder ESR spectra of **1a**, **1b** shown in Figures 4a and 4b are snapshots of the ESR characteristics that were displayed when the temperature was changed. The general morphology of the ESR lineshape remains unchanged, despite of the mentioned marked spectral-detailed changes, however, at lower temperature there was an increase of the signals, due to the peaks implying a decreasing in the branch mobility. It is noteworthy that at 77 K, the ESR linewidth spectra increased 19% for **1a** and 20% for **1b**, when comparing with the spectra at 300 K. This behaviour is explained by the spin-lattice relaxation mechanisms for flexible macromolecules, dipolar spread and the hyperfine interactions for paramagnetic compounds [56,57].

According to Mabbs [53], the coincidence of the principal values of the \hat{g} and \hat{A} tensors depend on the point symmetry at the metal. Considering the relationship among the \hat{g} and \hat{A} tensors, the symmetry point of paramagnets and the type of ESR spectrum, it can be concluded that the local symmetry around the Cu^{II} ion for **1a** is $<T$ where all the tensor axes are coincident $g_{xx}=g_{yy}=g_{zz}$, $A_{xx}=A_{yy}=A_{zz}$, and for **1b**, the Cu^{II} local symmetry is $<D_{3h}$, with tensor axes $g_{xx} \neq g_{yy} \neq g_{zz}$, $A_{xx} \neq A_{yy} \neq A_{zz}$. The point symmetry for **1b** is agree with the results obtained in the UV-Vis and X-ray measurements.

It is important to observe that the ESR spectra of **1a** and **1b** samples in solutions at different concentrations showed the same ESR singlet spectrum with *g* values, modified by $\Delta g \leq 0.013$ when the concentration was changed (Figure 5a, b).

Both spectra did not show hyperfine interaction, indicating dominant dipolar interactions. The fact that in solid ESR studies were different for **1a** and **1b**, but the spectra in solution became similar confirmed that **1a** and **1b** are two different crystalline phases with the same molecular structure.

DPPH free radical scavenging assay to prove biological activity

DPPH radical is commonly used as a radical molecule to evaluate the free radical scavenging capacity of several chemicals. The DPPH is characterized by a signal at 514 nm by UV-Vis, and it is able easily to accept an electron or hydrogen atom (proton) to become a stable diamagnetic molecule. Antioxidants, in the other hand, easily donate hydrogens to DPPH, in our case this role is played by the donation of an electron by Cu^{II}. Thus, the loss of the DPPH transition signal intensity in the presence of antioxidants is clearly directly proportional with the concentration (or number) of protons accepted. As shown in Figure 6, **1a** and **1b** were able to rapidly suppress the signal intensity after addition of the [Cu^{II}]₂(thb) in concentration dependent manner. As negative control, we analyze the free ligand at 0.1 mM giving no inhibition at all of the DPPH activity.

The DPPH assay proved the scavenging skill of both phases of [Cu^{II}]₂(thb)], however, to test the real strength of them we calculated the IC₅₀, which define the concentration needed to diminish certain activity at its half. An antioxidant reference is the Vitamin E analog, Trolox, which is already in the market. By comparing the IC₅₀ [Cu^{II}]₂

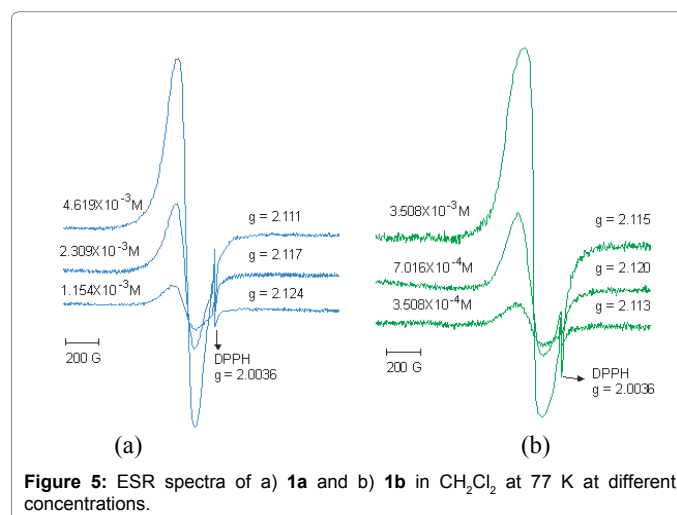


Figure 5: ESR spectra of a) **1a** and b) **1b** in CH₂Cl₂ at 77 K at different concentrations.

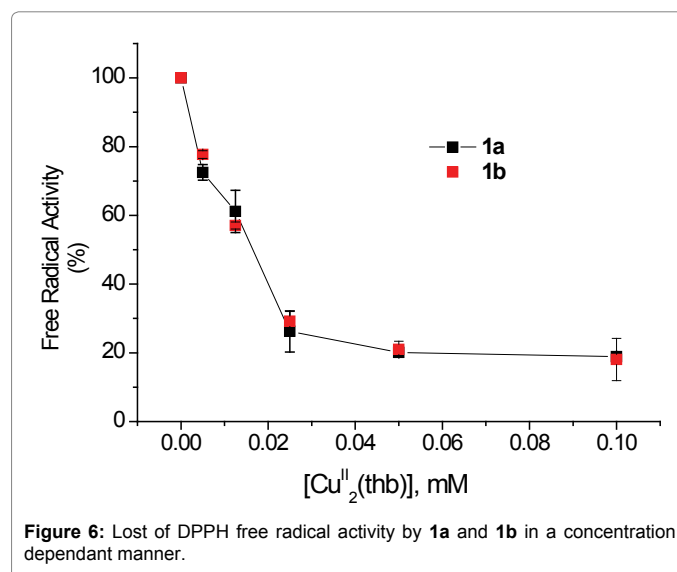


Figure 6: Lost of DPPH free radical activity by **1a** and **1b** in a concentration dependant manner.

(thb)] = 16.5 μ M versus the IC₅₀ Trolox = 36.9 μ M in undebatable that [Cu^{II}(thb)] is strong as Trolox inhibition wise.

Mechanism of scavenging by [Cu(thb)] 1a, 1b

In order to justify the loss of the free electron in the DPPH, **1a/1b** must be able to gain it. We followed this reduction process from Cu^{II} \rightarrow Cu^I by UV-Vis, Figure 7a and b. As we detailed above, the d_{xz}^2 , $d_{yz}^2 \rightarrow d_z^2$, $d_{x-y}^2 \rightarrow d_z^2$ and $d_{xy} \rightarrow d_z^2$ transitions for **1a/1b** appear around 810 nm (Supplementary Information, in Figure S8). The increase of DPPH concentration from 0.2 to 0.3 mM fade away the *d-d* transitions. This evidence describe that the scavenging compound is positively the Cu^{II} ions of **1a** and **1b**.

Conclusion

The spatial, electronic and magnetic measurements in solid and solution samples allowed us to conclude that two different crystalline phases **1a** and **1b** were obtained. The crystalline structure of **1b** is one of the first obtained for branched molecules, to our knowledge, and showed that **1b** consist of a dinuclear complexes, where the Cu ions are separated by a hydrocarbonated chain. Therefore, the magnetic data could be fitted by the Curie-Weiss and modified Curie-Weiss models, both models. Both models are adequate for complexes without exchange interactions. The above was confirmed by the ESR spectra, which showed *g* values \sim 2.1 for both phases, which is consistent with a spin state $s = 1/2$. For solid samples of **1a** and **1b**, the ESR spectra are completely different; in solution, both spectra were similar. The antioxidant activity of **1a** and **1b** was observed in UV-Vis spectra by the DPPH free radical scavenging assay showing a decreasing in the forbidden bands *d-d* and quantifying its capacity as IC₅₀ [Cu^{II}(thb)] = 16.5 μ M respect to IC₅₀ Trolox = 36.9 μ M. Both compounds gave the same antioxidant behavior observed through the UV-Vis spectra DPPH test, proving that **1a** and **1b** are the same molecules with crystalline arrangements. Structurally, the intermediate *sp* and *thp* geometries give possibilities to the DPPH to approach enough, allowing the free electron to be transferred into the Cu^{II} centre. Electronically, it is confirmed that the Cu^{II} reduction occurs in the d_z^2 orbital, being the highest energetically and the only one available to accept one electron, moreover, d_z^2 has the ideal geometry to make it possible. Magnetically, the ions communication is almost null, characteristic that should be noted. The spectroscopic and magnetic studies of the novel Cu^{II}-polymers, **1a** and **1b**, provide much information about the electronic, magnetic and spatial structures and its correlation with the antioxidant activity, being the more important contribution of this paper.

Acknowledgements

Secretaría de Educación Pública, Subsecretaría de Educación Superior, and Vicerrectoría de Investigación y Estudios de Posgrado from BUAP, Project

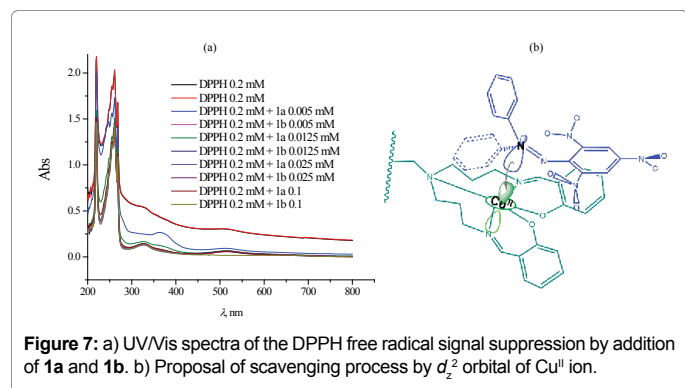


Figure 7: a) UV/Vis spectra of the DPPH free radical signal suppression by addition of **1a** and **1b**. b) Proposal of scavenging process by d_z^2 orbital of Cu^{II} ion.

REOY-NAT11, 12/2011, 2012-1, have supported this work. The authors are grateful to Dr. Sylvain Bernès (Universidad Autónoma de Nuevo León, México) for his participation in discussions on the correlation between spatial structure and magnetic behaviour and Dr. Roberto Escudero (Instituto de Investigaciones de Materiales, UNAM) for the magnetic measurements.

References

- Tomalia DA, Fréchet JMJ (2002) Discovery of Dendrimers and Dendritic Polymers: A Brief Historical Perspective. J Polym Sci Part: Polym Chem 40: 2719-2728.
- Tomalia DA, Naylor AM, Goddard III WA (1990) Starburst Dendrimers: Molecular-Level Control of Size, Shape, Surface Chemistry, Topology, and Flexibility from Atoms to Macroscopic Matter Angew. Chem Int Ed Engl 29: 138-175.
- Deng XX, Du FS, Li ZC (2014) Combination of Orthogonal ABB and ABC Multicomponent Reactions toward Efficient Divergent Synthesis of Dendrimers with Structural Diversity. Macro Lett 3: 667-670.
- Fu F, Wu Y, Zhu J, Wen S, Shen M, et al. (2014) Multifunctional lactobionic acid-modified dendrimers for targeted drug delivery to liver cancer cells: investigating the role played by PEG spacer. ACS Appl Mater Interfaces 6: 16416-16425.
- Sharma A, Mejia D, Regnaud A, Uhlig N, Li CJ, et al. (2014) Combined A3 Coupling and Click Chemistry Approach for the Synthesis of Dendrimer-Based Biological Tools. Macro Lett 3: 1079-1083.
- Hatano K, Matsubara T, Muramatsu Y, Ezure M, Koyama T, et al. (2014) Synthesis and influenza virus inhibitory activities of carbosilane dendrimers peripherally functionalized with hemagglutinin-binding Peptide. J Med Chem 57: 8332-8339.
- Crooks RM, Zhao M, Sun L, Chechik V, Yeung LK (2001) Dendrimer-encapsulated metal nanoparticles: synthesis, characterization, and applications to catalysis. Acc Chem Res 34: 181-190.
- Mitran E, Dellienger B, McCarley R (2010) Highly Size-Controlled, Low-Size-Dispersity Nickel Nanoparticles from Poly(propylene imine) Dendrimer-Ni(II) Complexes. Chem Matter 22: 6555-6563.
- Umeda Y, Kojima C, Harada A, Horinaka H, Kono K (2010) PEG-attached PAMAM dendrimers encapsulating gold nanoparticles: growing gold nanoparticles in the dendrimers for improvement of their photothermal properties. Bioconjug Chem 21: 1559-1564.
- Zhao M, Sun L, Crooks RM (1998) Preparation of Cu Nanoclusters within Dendrimer Templates. J Am Chem Soc 120: 4877-4878.
- Balogh L, Tomalia AT (1998) Poly(Amidoamine) Dendrimer-Templated Nanocomposites. 1. Synthesis of Zerovalent Copper Nanoclusters. J Am Chem Soc 120: 7355-7356.
- Floriano PN, Noble CO 4th, Schoonmaker JM, Poliakoff ED, McCarley RL (2001) Cu(0) nanoclusters derived from poly(propylene imine) dendrimer complexes of Cu(II). J Am Chem Soc 123: 10545-10553.
- Bingwa N, Meijboom R (2014) Kinetic Evaluation of Dendrimer-Encapsulated Palladium Nanoparticles in the 4-Nitrophenol Reduction Reaction. J Phys Chem C 118: 19849-19858.
- Deraedt C, Pinaud N, Astruc D (2014) Recyclable catalytic dendrimer nanoreactor for part-per-million Cu(I) catalysis of "click" chemistry in water. J Am Chem Soc 136: 12092-12098.
- Lo SC, Burn PL (2007) Development of dendrimers: macromolecules for use in organic light-emitting diodes and solar cells. Chem Rev 107: 1097-1116.
- Tran ML, Gahan LR, Gentle IR (2004) Structural Studies of Copper(II)-Amine Terminated Dendrimer Complexes by EXAFS. J Phys Chem B 108: 20130-20136.
- Tarazona-Vasquez F, Balbuena PB (2005) Complexation of Cu(II) Ions with the lowest generation poly(amido-amine)-OH dendrimers: a molecular simulation study. J Phys Chem B 109: 12480-12490.
- Amama PB, Maschmann MR, Fisher TS, Sands TD (2006) Dendrimer-templated Fe nanoparticles for the growth of single-wall carbon nanotubes by plasma-enhanced CVD. J Phys Chem B 110: 10636-10644.
- Cervantes-Mejía V, Baca-Solis E, Caballero-Jiménez J, Merino-García R, Moreno-Martínez G, et al. (2014) Branched Polyamines Functionalized with Proposed Reaction Pathways Based on 1H-NMR, Atomic Absorption and IR

- Spectroscopies. *Am J Analytical Chem* 5: 1090-1101.
20. Sompam P, Phisalaphong C, Nakornchai S, Unchern S, Morales NP (2007) Comparative antioxidant activities of curcumin and its demethoxy and hydrogenated derivatives. *Biol Pharm Bull* 30: 74-78.
 21. Morales NP, Sirirajoonwong S, Yamanont P, Phisalaphong C (2015) Electron Paramagnetic Resonance Study of the Free Radical Scavenging Capacity of Curcumin and Its Demethoxy and Hydrogenated Derivatives. *Biol Pharm Bull* 38: 1478-1483.
 22. Pacher P, Beckman JS, Liaudet L (2007) Nitric oxide and peroxynitrite in health and disease. *Physiol Rev* 87: 315-424.
 23. Sánchez-Sandoval A, Álvarez-Toledano C, Gutiérrez-Pérez R, Reyes-Ortega Y (2003) A Modified Procedure for the Preparation of Linear Polyamines. *Synth Commun* 33: 481-492.
 24. Gamosvkii AD, Karhisov BI, Gojon-Zorrilla G, Garnovskii DA (1995) Direct synthesis of coordination compounds from zerovalent metals and organic ligands. *Russian Chem Rev* 64: 201-221.
 25. Oxford Diffraction (2007) CrysAlis CCD and CrysAlis RED. Oxford Diffraction Ltd, Abingdon, England.
 26. Clark RC, Reid JS (1995) The Analytical Calculation of Absorption in Multifaceted Crystals. *Acta Cryst A* 51: 887-897.
 27. Sheldrick GM (1997) SHELXS97 and SHELXL97. University of Göttingen, Germany.
 28. Farrugia LJ (1997) ORTEP-3 for Windows - a version of ORTEP-III with a Graphical User Interface (GUI). *J Appl Cryst* 30: 565.
 29. Farrugia L (1999) WinGX Suite for Small-Molecule Single-Crystal Crystallography. *J Appl Cryst* 32: 837-838.
 30. Gutiérrez R, Vázquez J, Vázquez RA, Reyes Y, Toscano RA, et al. (2001) Chiral Complexes by Direct Synthesis of a Biomolecule and Metal Powders. Crystal Structures of the Dichloro[(-)-Sparteine-*N,N'*]M(II) Complexes (M = Cu, Zn). *J Coord Chem* 54: 313-321.
 31. Reyes-Ortega Y, Alcántara-Flores JL, Hernández-Galindo MC, Ramírez-Rosales D, Bernès S, et al. (2005) Magnetic Properties and Crystal Structure of a One-Dimensional Phase of Tetrakis(μ_2 -benzoato-*O,O'*)-bis(dimethyl sulfoxide)dicopper(II). *J Am Chem Soc* 127: 16312-16317.
 32. Addison AW, NageswaraRao T, Reedijk J, Van Rijn J, Verschoor GC (1984) Synthesis, structure, and spectroscopic properties of copper(II) compounds containing nitrogen-sulphur donor ligands; the crystal and molecular structure of aqua[7-bis(N-methylbenzimidazol-2'-yl)-2,6-dithiaheptane]copper(II) perchlorate. *J Chem Soc Dalton Trans* 1349-1356.
 33. Tercero J, Diaz C, Ribas J, Mahía J, Maestro MA (2002) New oxamato-bridged trinuclear Cu(II)-Cu(II)-Cu(II) complexes with hydrogen-bond supramolecular structures: synthesis and magneto-structural studies. *Inorg Chem* 41: 5373-5381.
 34. Chen ZL, Jiang CF, Yan WH, Liang FP, Batten SR (2009) Three-dimensional metal azide coordination polymers with amino carboxylate coligands: synthesis, structure, and magnetic properties. *Inorg Chem* 48: 4674-4684.
 35. Park G, Shao J, Lu FH, Rogers RD, Chasteen ND, et al. (2001) Copper(II) complexes of novel N-alkylated derivatives of cis,cis-,3,5-triaminocyclohexane. 1. Preparation and structure. *Inorg Chem* 40: 4167-4175.
 36. Lever ABP (1968) *Inorganic electronic spectroscopy*. Elsevier Pub, Amsterdam.
 37. Colthup NB, Daly LH, Wiberley SE (1990) *Introduction to Infrared and Raman Spectroscopy*. Academic Press, USA.
 38. Nakamoto K (1963) *Infrared Spectra of Inorganic and Coordination Compounds*. John Wiley & Sons Inc, New York.
 39. Alcántara-Flores JL, Ramírez-Rosales D, Bernès S, Ramírez-Bokhimi JG, Durán-Hernández A, et al. (2004) Synthesis and magnetostructural properties of two crystalline phases of [CuBr2(sp)] (sp=(-)-sparteine). *J Mol Struct* 693: 125-131.
 40. Reyes-Ortega Y, Alcántara-Flores JL, Hernández-Galindo MC, Gutiérrez-Pérez R, Ramírez-Rosales D, et al. (2006) Weak ferromagnetic behavior, crystal structure, and electronic studies of novel [Cu(II)(Br)(PhCO2)(Sp)] (Sp=(-)-sparteine) complex. *J Mol Struct* 788: 145-151.
 41. Quintero-Téllez MG, Rosales-Hoz MJ, Bernès S, Zamorano-Ulloa R, Ramírez-Rosales D, et al. (2013) Synthesis, structural, electronic and magnetic studies of [Cu(II)(salaenN3H3)]. *J Mol Struct* 1034: 183-188.
 42. Bertini I, Ciurli S, Dikiy A, Gasanov R, Luchinat C, et al. (1999) High-Field NMR Studies of Oxidized Blue Copper Proteins: The Case of Spinach Plastocyanin. *J Am Chem Soc* 121: 2037-2046.
 43. Godziela GM, Goff HM (1986) Solution characterization of copper(II) and silver(II) porphyrins and the one-electron oxidation products by nuclear magnetic resonance spectroscopy. *J Am Chem Soc* 108: 2237-2243.
 44. Dugad LB, Mitra S (1984) Nuclear Magnetic Resonance of paramagnetic Metalloporphyrins. *Proc Indian Acad Sci (Chem Sci)* 93: 295-311.
 45. Chandramouli GVR, Balagopalakrishna C, Rajasekharan MV, Manoharan PT (1996) Fitting of magnetic susceptibility data as a function of temperature of various spin systems-A FORTRAN program. *Computers Chem* 20: 353-358.
 46. Bonner JC, Fisher ME (1964) Linear magnetic chains with anisotropic coupling. *Phys Rev* 135: 640-658.
 47. Myers BE, Berger L, Friedberg SA (1969) Low Temperature Magnetization of Cu(NO3)2·2.5H2O. *J Appl Phys* 40: 1149-1151.
 48. Bleaney B, Bowers KD (1952) Anomalous Paramagnetism of Copper Acetate. *Proc R Soc London A* 214: 451-454.
 49. Drago RS (1992) *Physical Methods in Chemistry*. Saunders College Publishing, EUA.
 50. Cosio-Castañeda C, De la Mora P, Morales F, Escudero R, Tavizon G (2013) Magnetic behavior of the Bi2-ySryIr2O7 pyrochlore solid solution. *J Solid State Chem* 200: 49-53.
 51. Taira N, Wakeshima M, Hinatsu Y (2002) Magnetic susceptibility and specific heat studies on heavy rare earth ruthenate pyrochlores R2Ru2O7 (R = Gd-Yb). *J Mater Chem* 12: 1475-1479.
 52. Shannon N (2002) Mixed valence on a pyrochlore lattice-LiV2O4 as a geometrically frustrated magnet. *Eur Phys J B* 27: 527-540.
 53. Ottaviani MF, Montalti F, Turro NJ, Tomalia DA (1997) Characterization of Starburst Dendrimers by the EPR Technique. Copper(II) Ions Binding Full-Generation Dendrimers. *J Phys Chem B* 101: 158-166.
 54. Ottaviani MF, Bossmann S, Turro NJ, Tomalia DA (1994) Characterization of Starburst Dendrimers by the EPR Technique. 1. Copper Complexes in Water Solution. *J Am Chem Soc* 116: 661-671.
 55. Fehér G (1969) *Electron Paramagnetic Resonance with Applications to Selected Problems in Biology*. Gordon and Breach, New York.
 56. Weltner W (1983) *Magnetic Atoms and Molecules*. Dover Publications Inc., New York, USA.
 57. Mabbs FE (1993) *Some Aspects of the Electron Paramagnetic Resonance Spectroscopy of d-Transition Metal Compounds*. *Chem Soc Rev* 22: 313-324.